

CHIP Protects from the Neurotoxicity of Expanded and Wild-type Ataxin-1 and Promotes Their Ubiquitination and Degradation^{*[S]}

Received for publication, February 21, 2006, and in revised form, July 5, 2006 Published, JBC Papers in Press, July 10, 2006, DOI 10.1074/jbc.M601603200

Ismael Al-Ramahi^{‡§}, Yung C. Lam[¶], Hung-Kai Chen[‡], Beatrice de Gouyon[‡], Minghang Zhang[‡], Alma M. Pérez[‡], Joana Branco^{‡1}, Maria de Haro^{‡§}, Cam Patterson^{||}, Huda Y. Zoghbi^{¶¶**2}, and Juan Botas^{‡3}

From the [‡]Departments of Molecular and Human Genetics and [¶]Neuroscience, ^{**}Howard Hughes Medical Institute, Baylor College of Medicine, Houston, Texas 77030, the ^{||}Carolina Cardiovascular Biology Center and Departments of Medicine, Pharmacology, and Cell and Developmental Biology, University of North Carolina, Chapel Hill, North Carolina 27599, and the [§]Departamento de Biología, Facultad de Ciencias-University Autonoma de Madrid, Madrid 28049, Spain

CHIP (C terminus of Hsc-70 interacting protein) is an E3 ligase that links the protein folding machinery with the ubiquitin-proteasome system and has been implicated in disorders characterized by protein misfolding and aggregation. Here we investigate the role of CHIP in protecting from ataxin-1-induced neurodegeneration. Ataxin-1 is a polyglutamine protein whose expansion causes spinocerebellar ataxia type-1 (SCA1) and triggers the formation of nuclear inclusions (NIs). We find that CHIP and ataxin-1 proteins directly interact and co-localize in NIs both in cell culture and SCA1 postmortem neurons. CHIP promotes ubiquitination of expanded ataxin-1 both *in vitro* and in cell culture. The Hsp70 chaperone increases CHIP-mediated ubiquitination of ataxin-1 *in vitro*, and the tetratricopeptide repeat domain, which mediates CHIP interactions with chaperones, is required for ataxin-1 ubiquitination in cell culture. Interestingly, CHIP also interacts with and ubiquitinates unexpanded ataxin-1. Overexpression of CHIP in a *Drosophila* model of SCA1 decreases the protein steady-state levels of both expanded and unexpanded ataxin-1 and suppresses their toxicity. Finally we investigate the ability of CHIP to protect against toxicity caused by expanded polyglutamine tracts in different protein contexts. We find that CHIP is not effective in suppressing the toxicity caused by a bare 127Q tract with only a short hemagglutinin tag, but it is very efficient in suppressing toxicity caused by a 128Q tract in the context of an N-terminal huntingtin backbone. These data underscore the importance of the protein framework for modulating the effects of polyglutamine-induced neurodegeneration.

Polyglutamine (poly-Q)⁴ diseases are a group of neurodegenerative disorders caused by expansion of glutamine-encoding

(CAG)_n repeats in genes whose sequence is otherwise unrelated (1, 2). One such protein is ataxin-1, where expansion of its N terminus glutamine repeat triggers spinocerebellar ataxia type 1. SCA1 is an adult-onset disorder characterized by loss of motor coordination and balance, which progresses to affect vital brain functions such as breathing and swallowing. Brain dysfunction is in part due to degeneration of cerebellar Purkinje cells, brainstem neurons, and the spinocerebellar tracts. Strong evidence supports the idea of a gain of function mechanism triggered by the poly-Q expansion in ataxin-1 (1, 3–5).

One pathological hallmark of poly-Q disorders is the presence of neuronal aggregates (nuclear or cytoplasmic) that contain the poly-Q-expanded protein. These aggregates are found as nuclear inclusions (NIs) in SCA1 neurons, and in addition to aggregated mutant ataxin-1, they also contain components of the protein quality control machinery, *e.g.* ubiquitin, proteasome subunits, and chaperones. Such quality control proteins are key players in the toxicity of ataxin-1 and other proteins involved in poly-Q diseases (6–9).

Interestingly, high levels of unexpanded ataxin-1 form NIs and cause degenerative phenotypes similar to, but milder than, the phenotypes induced by expanded ataxin-1 both in *Drosophila* and mouse SCA1 models (10). Overexpression of either a human ataxin-1 deletion construct lacking the poly-Q repeat or *dAtx1* (the *Drosophila* ataxin-1 orthologue, which also lacks the N-terminal poly-Q tract) have been found to cause toxicity in two different fly models (3, 11). Taken together these observations suggest that poly-Q expansion favors a toxic and aggregation-prone conformation in ataxin-1 that the protein backbone may already have a tendency to adopt.

Chaperones and the ubiquitin proteasome system are responsible for maintaining the cell environment free of toxic misfolded proteins (12, 13). Although not well understood, there is a tight regulatory mechanism that decides when a protein is refolded and when it needs to be degraded. One link that

^{*} This work was supported in part by National Institutes of Health Grants NS42179 (to J. B.) and NS27699 (to H. Y. Z.). The costs of publication of this article were defrayed in part by the payment of page charges. This article must therefore be hereby marked "advertisement" in accordance with 18 U.S.C. Section 1734 solely to indicate this fact.

^[S] The on-line version of this article (available at <http://www.jbc.org>) contains supplemental Figs. 1 and 2.

¹ Supported by the Portuguese Foundation for Science and Technology.

² A Howard Hughes Medical Institute Investigator.

³ To whom correspondence should be addressed. Tel.: 713-798-5937; Fax: 713-798-8142; E-mail: jbotas@bcm.tmc.edu.

⁴ The abbreviations used are: poly-Q, poly-glutamine; E1, ubiquitin-activating enzyme; E2, ubiquitin carrier protein; E3, ubiquitin protein ligase; Ub, ubiquitin; HA, hemagglutinin; SCA1, spinocerebellar ataxia type 1; SCA1^{7Q}, gene

coding for ataxin-1 [nQ] protein; NI, nuclear inclusion; CHIP, C-terminus of Hsc-70 interacting protein; TPR, tetratricopeptide repeat; GFP, green fluorescent protein; RT, reverse transcriptase; F-ataxin-1, FLAG-tagged ataxin-1; SEM, scanning electron microscopy; EID, eye imaginal disc; 127Q-HA, hemagglutinin-tagged glutamine 127; NT-Htt[128Q], glutamine 128-expanded N-terminal huntingtin; co-IP, co-immunoprecipitation; MOPS, 4-morpholinepropanesulfonic acid; PBS, phosphate-buffered saline.

connects chaperones and the ubiquitin-proteasome machinery, possibly acting as a regulator, is the co-chaperone CHIP (C terminus of Hsc70 interacting protein) (14, 15).

CHIP has three tetratricopeptide repeat (TPR) domains that allow it to interact with chaperones (16), as well as a U-box domain that confers this co-chaperone with an E3 ubiquitin ligase activity (17). CHIP has been shown to work in the protein quality control machinery at different levels. It can induce the degradation of misfolded proteins (14, 15, 18, 19). CHIP can also cause increased refolding of non-native proteins in an Hsp70-dependent manner (20) and activates heat shock factor 1 improving the stress tolerance in cells (21).

CHIP is known to interact with aggregation-prone proteins implicated in degenerative diseases protecting against their toxicity. Among these proteins are superoxide dismutase, Tau, poly-Q-expanded ataxin-3, poly-Q-expanded N-terminal huntingtin, and α -synuclein (22–29).

Given the ability of CHIP to recognize and protect against aberrantly folded proteins, we tested its ability to suppress ataxin-1-induced neurodegeneration and used it as a tool to investigate the surprising toxicity observed in unexpanded ataxin-1. Here we report that: 1) CHIP is able to interact with both expanded and unexpanded ataxin-1 proteins and targets them for degradation by promoting their ubiquitination. 2) CHIP localizes to ataxin-1 NIs in cultured cells and human SCA1 neurons. 3) Increased CHIP activity suppresses neurodegeneration triggered by either expanded or unexpanded ataxin-1 by reducing their steady-state levels in a *Drosophila* model of SCA1. 4) Finally we investigate the importance of the protein backbone for CHIP neuroprotection. We find that CHIP has little protection activity against the toxicity caused by a pure poly-Q tract but is very effective in protecting against a similar poly-Q tract in the context of a protein backbone.

EXPERIMENTAL PROCEDURES

In Vitro Ubiquitination Assays—Bacterially expressed ataxin-1 [2Q] or [82Q] (0.25 μ g) was incubated in reactions containing 0.1 μ M purified rabbit E1 (Calbiochem), 8 μ M UBCH5a, 4 μ M CHIP, 2.5 mg/ml ubiquitin (Sigma), 5 mM ATP in 20 mM MOPS, pH 7.2, 100 mM KCl, 5 mM MgCl₂, 10 mM dithiothreitol, 1 mM phenylmethylsulfonyl fluoride for 2 h at 30 °C. In some reactions, 2 μ M Hsp70 was included. Reactions were stopped with SDS loading buffer and subjected to SDS-PAGE, then immunoblotted with anti-ataxin-1 antibody.

Co-immunoprecipitation and in Vivo Ubiquitination—HeLa cells were cultured in Dulbecco's modified Eagle's medium supplemented with 10% fetal bovine serum (5% CO₂). Transfections of FLAG-tagged ataxin-1 2Q, 82Q, and human CHIP were performed using Lipofectamine 2000 (Invitrogen). Cells were lysed in TST extraction buffer (50 mM Tris-HCl, pH 7.5, 0.15 M NaCl, and 0.5% Triton X-100) containing protease inhibitors and subjected to immunoprecipitation with anti-FLAG-conjugated gel (Sigma) for 2 h at 4 °C.

For determining ataxin-1 ubiquitination *in vivo*, HeLa cells in 10-cm dishes were transfected with vectors expressing FLAG-tagged ataxin-1 [82Q] (6 μ g), human CHIP variants (wild-type; TPR mutant K30A; and U-box double mutant

D253N,R254G) (5 μ g) and/or hemagglutinin-tagged ubiquitin (5 μ g). After 24 h, the cells were treated with 50 μ M MG132 (Calbiochem) for 8 h and were lysed and subjected to immunoprecipitation with anti-FLAG-conjugated gel. Immunoprecipitates were washed with lysis buffer five times and were separated by SDS-PAGE and analyzed by Western blotting with appropriate antibodies. The antibodies used were as follows: rabbit polyclonal anti-ataxin-1 (11750VII) (1:3000), rabbit polyclonal anti-CHIP (1:2000), and mouse monoclonal anti-HA (Babco) and rabbit polyclonal anti-FLAG (Sigma).

Cell Culture Immunofluorescence—Transient expression of FLAG-tagged ataxin-1 and human CHIP in COS7 cells was accomplished by transfection with Lipofectamine 2000 in 6-well tissue culture plates containing sterile coverslips. Immunofluorescence staining was done as described in Ref. 7. Mouse monoclonal antibodies M2 anti-FLAG (1:500, Sigma) and/or rabbit anti-CHIP (1:500) were used. Subsequently, cells were incubated with either anti-mouse Alexa-488 conjugated (Molecular Probes) or anti-rabbit-Cy3 (The Jackson Laboratory) mounted in anti-fade solution (Vectashield mounting medium, Vector Laboratories) and analyzed by laser confocal microscopy (Bio-Rad 1024).

Drosophila Strains—The UAS-CHIP constructs were generated by cloning a cDNA coding for human CHIP in the pUAST *Drosophila* expression vector (30). Transgenic *Drosophila* lines were generated by injecting this construct in embryos following standard methods.

UAS-SCA1^{82Q} and UAS-SCA1^{30Q} strains have been described previously (10). Flies carrying UAS-127Q:HA (MGGPP-STPQ_nTSRTYPYDVPDYA) were a provided by Dr. P. Kazemi-Esfarjani. All other strains were obtained from the Bloomington Stock Center.

Western Blot Assays—For immunoblots from larval tissue, eye imaginal discs from 10 animals per genotype were dissected in PBS. Tissue was homogenized in 30 μ l of Laemmli sample buffer (Bio-Rad) and loaded on a 7.5% Tris-HCl Ready Gel (Bio-Rad). For adult tissues, five heads per genotype were homogenized and processed in the same way.

Membranes were stained with primary antibodies 11NQ anti-ataxin-1 (1:1000) and mouse anti-tubulin (Hybridoma Bank, 1:1000). Horseradish peroxidase-conjugated anti-mouse or anti-rabbit IgG secondary antibodies (1:5000; Bio-Rad) were used. Membranes were developed using a ECL Western blot detection kit (Amersham Biosciences).

Immunofluorescence Staining and Quantification on Drosophila Imaginal Discs—Eye imaginal discs from seven different larvae per genotype were dissected in PBS and fixed with 4% formaldehyde (in PBS) for 30 min. Primary antibodies 11NQ anti-ataxin-1 (1:1000) or 3E10 anti-GFP (1:200; Molecular Probes) were used. For the secondary antibody staining we used Alexa-488-tagged antibodies (1:200; Molecular Probes). Image acquisition and signal quantification were carried out following previously published procedures (31).

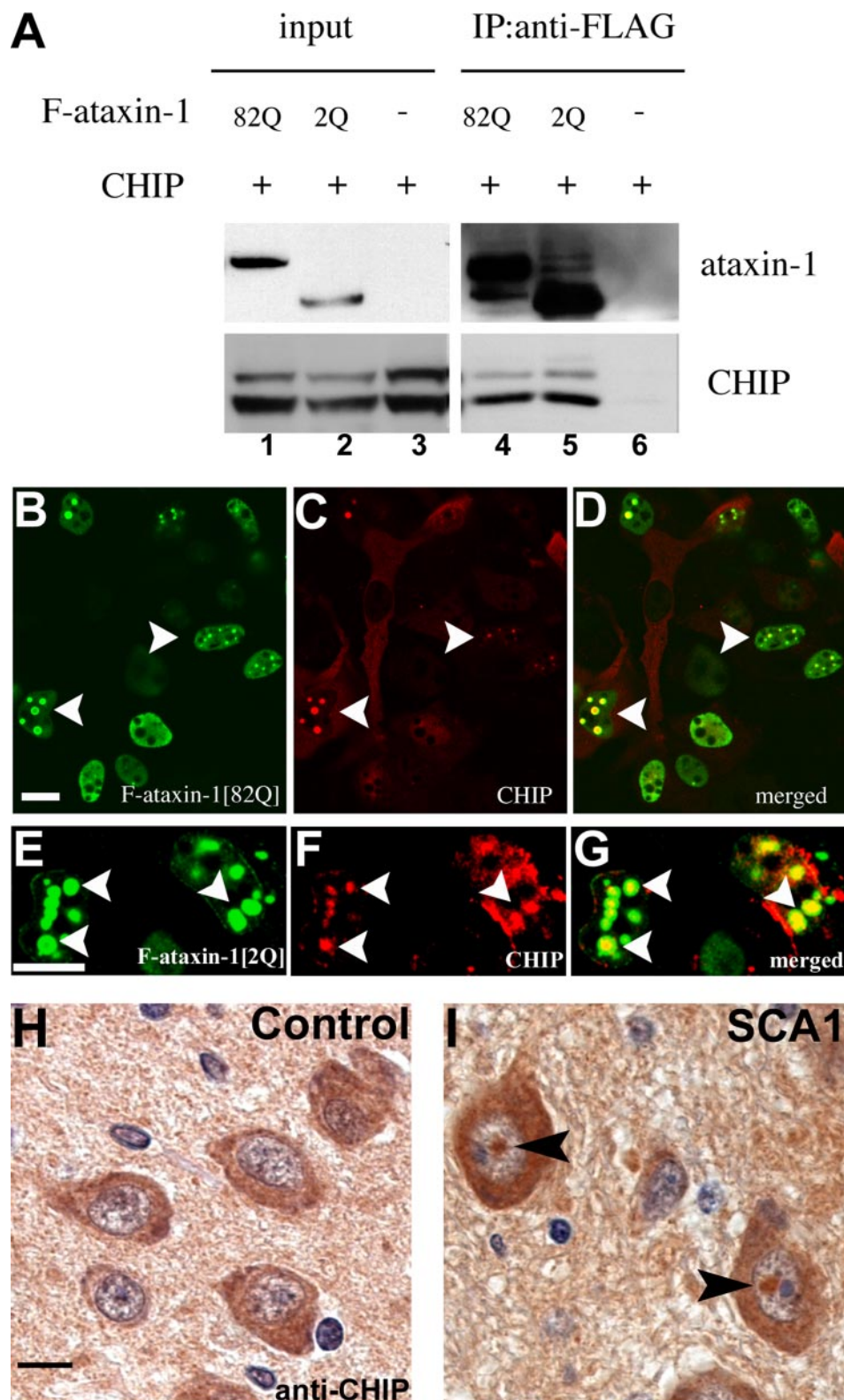
Immunohistochemical Staining of Human Brain Tissue—Brain tissue from a SCA1 autopsy and a non-SCA1 control was fixed in formol and embedded in paraffin. 5- μ m sections were obtained from the pons area of both brains and then

CHIP Degrades Ataxin-1 and Suppresses Its Toxicity

rehydrated to PBS. Slides were stained using primary antibody rabbit anti-human CHIP (1:200). Biotin anti-rabbit (Vector Laboratories) was used as a secondary antibody. Slides were developed using DAB/H₂O₂ after 1-h incubation in the Vectastain-ABCkit[Elite] (Vector Laboratories). Hematoxylin (Sigma) was used for counterstaining.

Scanning Electron Microscopy and Eye Paraffin Sections—Processing of *Drosophila* for scanning electron microscopy (SEM) and image acquisition were performed following previously published procedures (10).

For paraffin sections, flies were fixed with 4% formaldehyde (in PBS). Heads were dehydrated in increasing concentrations



of ethanol and embedded in paraffin. Ten- μ m serial sections were obtained and rehydrated to PBS. Sections were stained with hematoxylin (Sigma). Images were captured using an AxioCam MRc camera (Zeiss) attached to a Microphot-FXA microscope (Nikon).

Reverse Transcriptase-PCR—Total RNA from the imaginal eye discs of seven different larvae per genotype was extracted using the TRIzol reagent (Invitrogen) and treated with RNase-free DNase I (Invitrogen). Reverse transcription and PCR were conducted using Super-Script III First Strand Synthesis for RT-PCR kit with Platinum Taq (Invitrogen) following indications from the supplier. The number of cycles was optimized to allow a linear range of detection of transcripts. SCA1 transcripts were amplified along with transcripts for RP49, which served as an internal control. The primers used were as follows: SCA1, 5'-CTGCAGTTTGCGGC-TCTCT-3' and 5'-GAGCTAAAGAAGGTGGAAGACTT-AAA-3'; RP49, 5'-AAACGCGGTTCTGCATGAG-3' and 5'-GACGCTTCAAGGGACAGTATCTG-3'; and SV40, 5'-GGAACTGATGAATGGGAGCA-3' and 5'-GGAAAGTC-CTTGGGGTCTTC-3'.

RESULTS

CHIP Interacts with Expanded and Unexpanded Human Ataxin-1 in Cultured Cells—To assess whether CHIP and expanded ataxin-1 [82Q] interact, we performed co-immunoprecipitation (co-IP) assays. As shown in lane 4 of Fig. 1A, ataxin-1 [82Q] pulls down CHIP.

Overexpression of unexpanded ataxin-1 leads to neurodegenerative phenotypes in *Drosophila* and mouse models that are similar to, but milder than, the degeneration caused by ataxin-1 [82Q] (10). Prompted by this observation, we asked whether CHIP is able to interact with a wild-type ataxin-1 protein without the poly-Q expansion. We performed a co-IP assay with cells co-expressing CHIP and an ataxin-1 protein with only 2 glutamines (normal human ataxin-1 has 6–39 glutamines). Lane 5 in Fig. 1A shows that ataxin-1 [2Q] also pulls down CHIP. The finding that CHIP interacts with the ataxin-1 protein backbone supports the idea that even unexpanded ataxin-1 has a tendency to misfold.

The interaction between CHIP and ataxin-1 may be direct or mediated by chaperones that are known to interact with both CHIP and ataxin-1 in co-IP and other experiments (7, 10, 16, 17, 19, 31).

CHIP Localizes to Ataxin-1 Nuclear Inclusions in Cultured Cells and Neurons from SCA1 Brains—We used indirect immunofluorescence to determine whether CHIP and ataxin-1 co-

localize in cultured cells co-expressing CHIP and expanded ataxin-1. As shown in Fig. 1, B–D, CHIP accumulates in ataxin-1 [82Q] NIs formed in SCA1^{82Q}-expressing cells. This observation suggests that CHIP may have a role in the clearance of aggregated mutant ataxin-1 *in vivo*. CHIP also localizes to unexpanded ataxin-1 [2Q] NIs (Fig. 1, E–G), further supporting the idea that unexpanded ataxin-1 can adopt aberrant conformations.

To investigate whether the CHIP-ataxin-1 interactions described above are relevant for SCA1 pathology, we analyzed the distribution of endogenous human CHIP on pontine neurons from a SCA1 or control brain tissue. CHIP localizes to the cytoplasm in neurons of control brains and is not detected in the nucleus (Fig. 1H). In contrast, CHIP label was detected in 100% ($n = 102$) of the NIs present in the SCA1 brain tissue that we studied (Fig. 1I). Recruitment of CHIP to the NIs in SCA1 neurons suggests a role for CHIP in the clearance of expanded ataxin-1 in humans.

CHIP Ubiquitinates Both Expanded and Unexpanded Ataxin-1 *In Vitro*—The interactions between ataxin-1 and CHIP suggest that CHIP may promote ataxin-1 ubiquitination and target it for degradation. To test this possibility, we carried out *in vitro* ubiquitination experiments. Either ataxin-1 [82Q] or ataxin-1 [2Q] were incubated with the appropriate ubiquitination machinery components using CHIP as the E3 ligase. We found that CHIP promotes ubiquitination of both expanded and unexpanded ataxin-1 proteins (Fig. 2A), further suggesting that unexpanded ataxin-1 can adopt an aberrant conformation in the absence of the poly-Q expansion. In contrast, CHIP does not ubiquitinate a native control protein (luciferase) as shown in supplemental Fig. 1.

Hsp70 Enhances CHIP-mediated Ataxin-1 Ubiquitination *In Vitro*—Because Hsp70 modulates ataxin-1 [82Q] toxicity and is also known to interact with CHIP (7, 9, 10, 16), we investigated the effect of Hsp70 on CHIP-mediated ataxin-1 [82Q] ubiquitination. Hsp70 was added to the *in vitro* ubiquitination assay described above. The addition of Hsp70 results in increased ubiquitination of ataxin-1 [82Q] when compared with CHIP alone. A similar result was obtained for ataxin-1 [2Q] (Fig. 2B). Because Hsp70 interacts with misfolded proteins, these findings support the idea that a portion of unexpanded ataxin-1 [2Q] molecules adopts an aberrant conformation.

CHIP Mediates Ataxin-1 Ubiquitination in Cell Culture and Requires a Functional TPR Domain—In cells expressing SCA1^{82Q}, ataxin-1 ubiquitination is evident after incubation with the proteasome inhibitor MG-132 (Fig. 2C, lanes 1 and 2).

FIGURE 1. CHIP interacts with both expanded and unexpanded ataxin-1 and is recruited to ataxin-1 nuclear inclusions in cultured cells and SCA1 neurons. A, co-IP assays between FLAG-ataxin-1 [82Q] (F-ataxin-1) or F-ataxin-1 [2Q] and CHIP. Lanes 1–3 show the inputs from cells co-expressing CHIP and either FLAG-ataxin-1 [82Q] (lane 1), F-ataxin-1 [2Q] (lane 2), or an empty vector control (lane 3). The upper CHIP band corresponds to mono-ubiquitinated CHIP (C. Patterson, unpublished observation). CHIP is pulled down by both F-ataxin-1 [82Q] and F-ataxin-1 [2Q] (lanes 4 and 5, respectively), after anti-FLAG immunoprecipitation (IP). No CHIP is detected after immunoprecipitation in the negative control (lane 6). Ataxin-1 was detected with rabbit polyclonal anti-ataxin-1 (11750V7); CHIP was detected with rabbit polyclonal anti-CHIP. B–D, immunofluorescence staining in cells co-expressing F-ataxin-1 [82Q] (green) and CHIP (red). B, F-ataxin-1 [82Q] accumulates in NIs (arrowheads) in cultured cells. C and D, CHIP is recruited to F-ataxin-1 [82Q] nuclear inclusions. E–G, similar staining as B–D performed on cells expressing F-ataxin-1 [2Q] and CHIP. Notice that CHIP is also recruited to unexpanded ataxin-1 nuclear inclusions (arrowheads). H and I, paraffin sections of the pontine area of the brain from either a control or an SCA1 autopsy immunostained with anti-hCHIP antibody. H, CHIP staining is cytoplasmic in control pontine neurons and undetectable in nuclei. I, in addition to the cytoplasmic CHIP, pontine neurons from the SCA1 brain show intra-nuclear anti-CHIP staining in the form of NIs (arrowhead). A total of 102 neurons with NIs were studied and all of them were positive for CHIP. B–I, scale bars = 10 μ m. In control experiments in which SCA1 autopsy brain tissue was stained with secondary but no anti-CHIP primary antibody, the ataxin-1 NIs are clearly visible with the hematoxylin counter-stain (see supplemental Fig. 2).

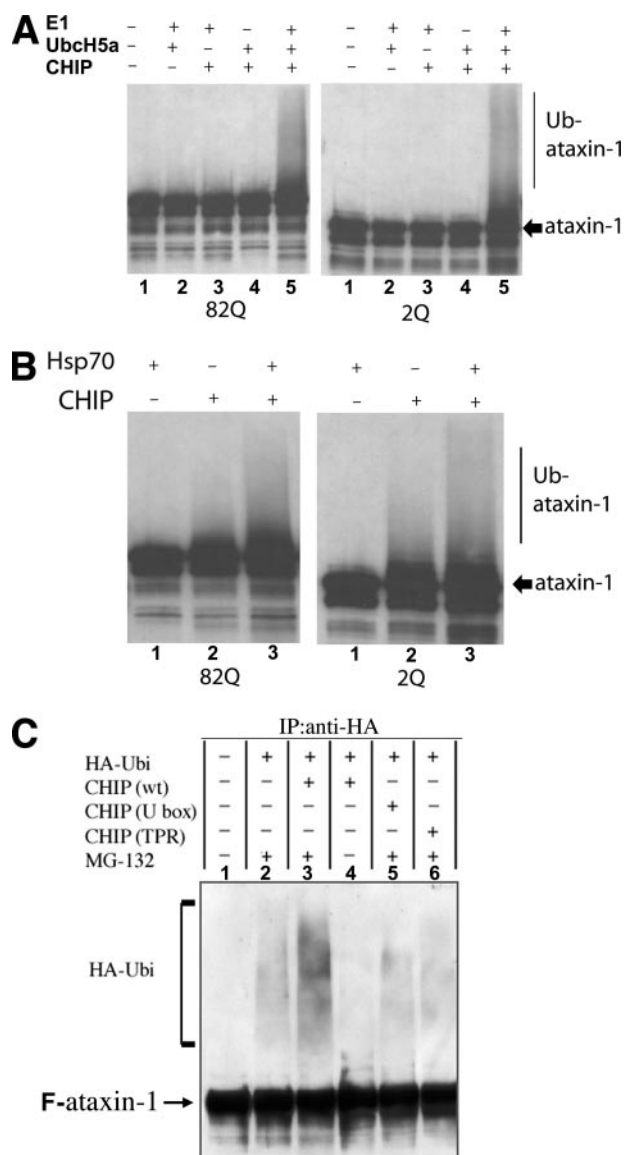


FIGURE 2. CHIP ubiquitinates both expanded and unexpanded ataxin-1. *A*, *in vitro* ubiquitination assay with either ataxin-1 [82Q] (left blot) or ataxin-1 [2Q] (right blot) and CHIP. Lane 1 in both blots shows no ubiquitinated ataxin-1 (Ub-ataxin-1) in the absence of any ubiquitination machinery components. Similarly, no ubiquitinated ataxin-1 is detected when lacking one of the following components, CHIP (E3), UbcH5a (E2), or rabbit E1 (lanes 2–4, respectively). Lane 5 in both blots shows a clear ubiquitination smear (Ub-ataxin-1) when all the ubiquitination machinery components are present in combination with either ataxin-1 [82Q] or ataxin-1 [2Q]. Blots were stained with rabbit polyclonal anti-ataxin-1 (11750Vil). *B*, *in vitro* ubiquitination assay with ataxin-1 [82Q] (left blot) or ataxin-1 [2Q] (right blot) and CHIP in the absence or presence of Hsp70. No ubiquitinated ataxin-1 (Ub-ataxin-1) is detected following incubation with Hsp70 alone (lane 1 in both blots). Some ubiquitinated ataxin-1 is detected after incubation with CHIP alone (lane 2 in both blots). Lane 3 in both blots shows increased ubiquitinated ataxin-1 when incubated with CHIP and Hsp70 simultaneously. *C*, *in vivo* ubiquitination assay in cells co-expressing F-ataxin-1 [82Q], hemagglutinin-Ubiquitin (HA-Ubi), and either normal CHIP (CHIP(wt), lane 3) or CHIP with a point mutation in its catalytic U-box (lane 5) or its tetratricopeptide (TPR, lane 6) domains. Lane 1, no ubiquitinated ataxin-1 (HA-Ubi) is detected in F-ataxin-1 [82Q] control cells. Lane 2 shows some ubiquitinated F-ataxin-1 [82Q] when cultured cells were treated with the proteasome inhibitor MG-132. Co-expression of CHIP(wt) and F-ataxin-1 [82Q] causes increased ataxin-1 [82Q] ubiquitination in MG-132 treated cells (lane 3). No ubiquitinated ataxin-1 [82Q] is detected in similar cells as lane 3 without the MG-132 treatment (lane 4). No increase in ubiquitinated ataxin-1 [82Q] is detected in F-ataxin-1 [82Q] cells co-expressing the U-box or TPR CHIP mutants (lanes 5 and 6, respectively). Immunoprecipitation of F-ataxin-1 was done with anti-FLAG-conjugated beads; the blot was jointly probed with anti-HA (Babco) and anti-FLAG (Sigma) antibodies.

The levels of ubiquitinated ataxin-1 are increased in cells simultaneously expressing *SCA1*^{82Q} and *CHIP* (Fig. 2C, lane 3). To investigate whether the U-box domain in CHIP is necessary for ataxin-1 ubiquitination *in vivo*, we used a mutant CHIP with a nonfunctional U-box domain (*CHIP*^{U-box}). Cells co-expressing *CHIP*^{U-box} and *SCA1*^{82Q} failed to show an increase in ataxin-1 ubiquitination when compared with cells expressing *SCA1*^{82Q} alone (Fig. 2C, lane 5). These results confirm our *in vitro* observations, indicate that CHIP is able to target ataxin-1 [82Q] for degradation *in vivo*, and are in accordance with the role of the U-box domain in providing an interface for interactions with the ubiquitin conjugase (32).

TPR domains in CHIP have been shown to interact with chaperones (16). We monitored ataxin-1 [82Q] ubiquitination in cells co-expressing *SCA1*^{82Q} and a *CHIP* construct with a nonfunctional TPR domain (*CHIP*^{TPR}). Lysates from these cells failed to show increased ataxin-1 ubiquitination when compared with those coming from cells expressing *SCA1*^{82Q} alone (Fig. 2C, lane 6). This observation suggests that interactions with chaperones are required for CHIP-mediated ataxin-1 [82Q] ubiquitination *in vivo*.

CHIP Suppresses the Toxicity of Expanded Ataxin-1 in a Drosophila Model of SCA1—The ubiquitination of ataxin-1 by CHIP and its co-localization in NIs in both cell culture and *SCA1* neurons suggest that CHIP may protect against ataxin-1-induced neurotoxicity.

To test this hypothesis we used a well characterized animal model of *SCA1*. We have previously shown that *SCA1*^{82Q} expression in the *Drosophila* eye causes a degenerative phenotype (10). The fly genome contains a *CHIP* orthologue for which no mutations are available. However, we compared the eye phenotype of flies co-expressing *SCA1*^{82Q} and a control transgene (*UAS-LacZ*) with the phenotype of flies expressing *SCA1*^{82Q} together with human *CHIP* (Fig. 3). Two *CHIP* transgenic lines were used for our analysis, one medium and one strong (referred to as *CHIP*m and *CHIP*s, respectively) based on the amount of *CHIP* protein being expressed (Fig. 4A). Flies co-expressing *SCA1*^{82Q} and *LacZ* show a severe external eye phenotype characterized by ommatidial disorganization and fusion as well as interommatidial bristle loss (Fig. 3, compare A and B). Internally, these eyes present severe retinal degeneration evident by reduction in the depth of the retina (Fig. 3, compare E and F). In contrast, eyes co-expressing *CHIP* and *SCA1*^{82Q} show a clear amelioration of the ommatidial disorganization (Fig. 3, C and D) as well as retinal phenotypes (Figs. 3, G and H). The extent of phenotype suppression is dependent on the amount of *CHIP* protein being co-expressed with ataxin-1 [82Q] as evidenced comparing the effects of *CHIP*s with *CHIP*m.

CHIP Overexpression Reduces the Levels of Expanded Ataxin-1 in Vivo—To further test the hypothesis that CHIP protects against *SCA1*-induced neurodegeneration by targeting ataxin-1 for degradation, we monitored the amounts of ataxin-1 [82Q] protein present in tissues expressing *SCA1*^{82Q} and different levels of *CHIP*.

First we monitored the levels of ataxin-1 [82Q] by Western blot analysis. Since substantial cell loss occurs in the adult eye due to *SCA1*^{82Q} expression, we used third instar eye imaginal

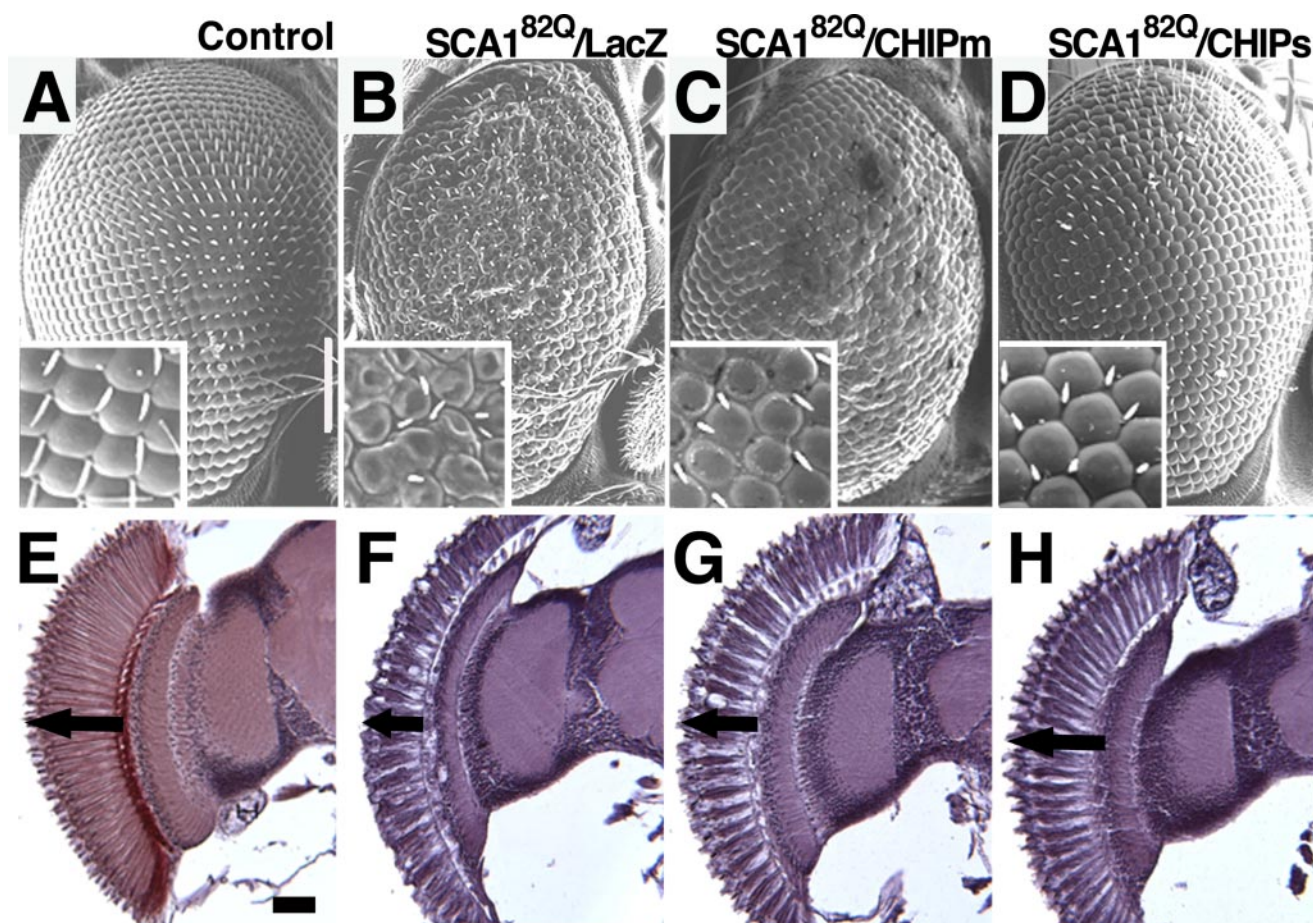


FIGURE 3. CHIP suppresses eye degeneration induced by expanded ataxin-1 in *Drosophila*. A, SEM images (A) and horizontal paraffin sections of fly eyes expressing *SCA1*^{82Q} and different levels of *CHIP* (genotype combinations indicated on top) (E–H) are shown. *SCA1*^{82Q}-expressing eyes present strong ommatidial disorganization and severe reduction in retinal depth when compared with controls (compare A with B and E with F). Combining *SCA1*^{82Q} with either a medium or a strong expressing *CHIP* line (*CHIPm* and *CHIPs*, respectively) suppresses the *SCA1*^{82Q}-induced external eye (compare C and D with B) and retinal phenotypes (compare G and H with F). Note that *CHIPs* is a better suppressor than *CHIPm* (compare C with D and G with H). Genotypes: A and E, *yw*; *gmr-GAL4/+*; B and F, *UAS-SCA1*^{82Q} [F7]/*yw*; *gmr-GAL4/UAS-LacZ*; C and G, *UAS-SCA1*^{82Q} [F7]/*yw*; *gmr-GAL4/+*; *UAS-CHIPm/+*; D and H, *UAS-SCA1*^{82Q} [F7]/*yw*; *gmr-GAL4/UAS-CHIPs*. Scale bar in A–D = 100 μ m; insets are 50 \times 50 μ m. Scale bar in E–H = 10 μ m. A–D, done at 27 $^{\circ}$ C. E–H, done at 25 $^{\circ}$ C.

discs to quantify ataxin-1 [82Q] levels. Less ataxin-1 [82Q] is detected in eye discs co-expressing *CHIP* and *SCA1*^{82Q} than in *SCA1*^{82Q}/*LacZ* controls. The decrease in the amount of ataxin-1 [82Q] inversely correlates to the amount of *CHIP* being expressed (Fig. 4B).

Because expanded ataxin-1 [82Q] forms insoluble aggregates, Western blots might only resolve the extractable protein fraction. To circumvent this limitation we also monitored the levels of ataxin-1 [82Q] by immunofluorescence analysis. This method allowed us to quantify both the soluble and the aggregated fractions of ataxin-1 [82Q]. Eye imaginal discs expressing *SCA1*^{82Q} and *CHIP* show a clear decrease in ataxin-1 [82Q] signal when compared with *SCA1*^{82Q}/*LacZ* controls after fluorescence quantification (Fig. 4, C–E and I). Like the Western blot data, this decrease was inversely correlated to the amount of *CHIP* protein being expressed.

These results might be explained if *CHIP* interferes with the *GAL4-UAS* system used to drive *SCA1*^{82Q} expression. To test this possibility we investigated whether *CHIP* modifies the amount of GFP expressed from a *UAS-GFP* control transgene. Quantification of GFP by immunofluorescence (Fig. 4, F–H and J) as well as Western blot analysis (data not shown) on eye discs

co-expressing GFP and different levels of *CHIP* failed to show a decrease in the amount of total GFP.

Finally, we tested the possibility that a *CHIP*-mediated decrease in the amount of ataxin-1 protein is caused by reduction of *SCA1* messenger RNA. We performed semiquantitative RT-PCR analysis using larval eye imaginal discs co-expressing either *SCA1*^{82Q} and *LacZ* or *SCA1*^{82Q} and *CHIPs*. The amounts of *SCA1*^{82Q} mRNA in the context of the *CHIPs* and *LacZ* transgenes are similar (Fig. 4K). Thus, the GFP and RT-PCR data show that the effects of *CHIP* on ataxin-1 [82Q] neurodegeneration are at the protein level.

CHIP Suppresses the Toxicity and Reduces the Levels of Unexpanded Ataxin-1—Since *CHIP* promotes ubiquitination of, and is pulled down by, ataxin-1 [2Q] (Fig. 2), we asked whether it is able to interact with unexpanded ataxin-1 *in vivo*. We investigated the effect of *CHIP* co-expression in flies carrying two different unexpanded human *SCA1* transgenes (*SCA1*^{30Q} and *SCA1*^{82Q}). The *SCA1*^{30Q} line expresses four times more protein than the *SCA1*^{82Q} line used above (data not shown). In these conditions, *SCA1*^{30Q} causes a moderate external eye phenotype at 29 $^{\circ}$ C (Fig. 5A) and a reduction in retinal depth similar to that caused by *SCA1*^{82Q} at 27 $^{\circ}$ C (Fig. 5E). The *SCA1*^{2Q} line

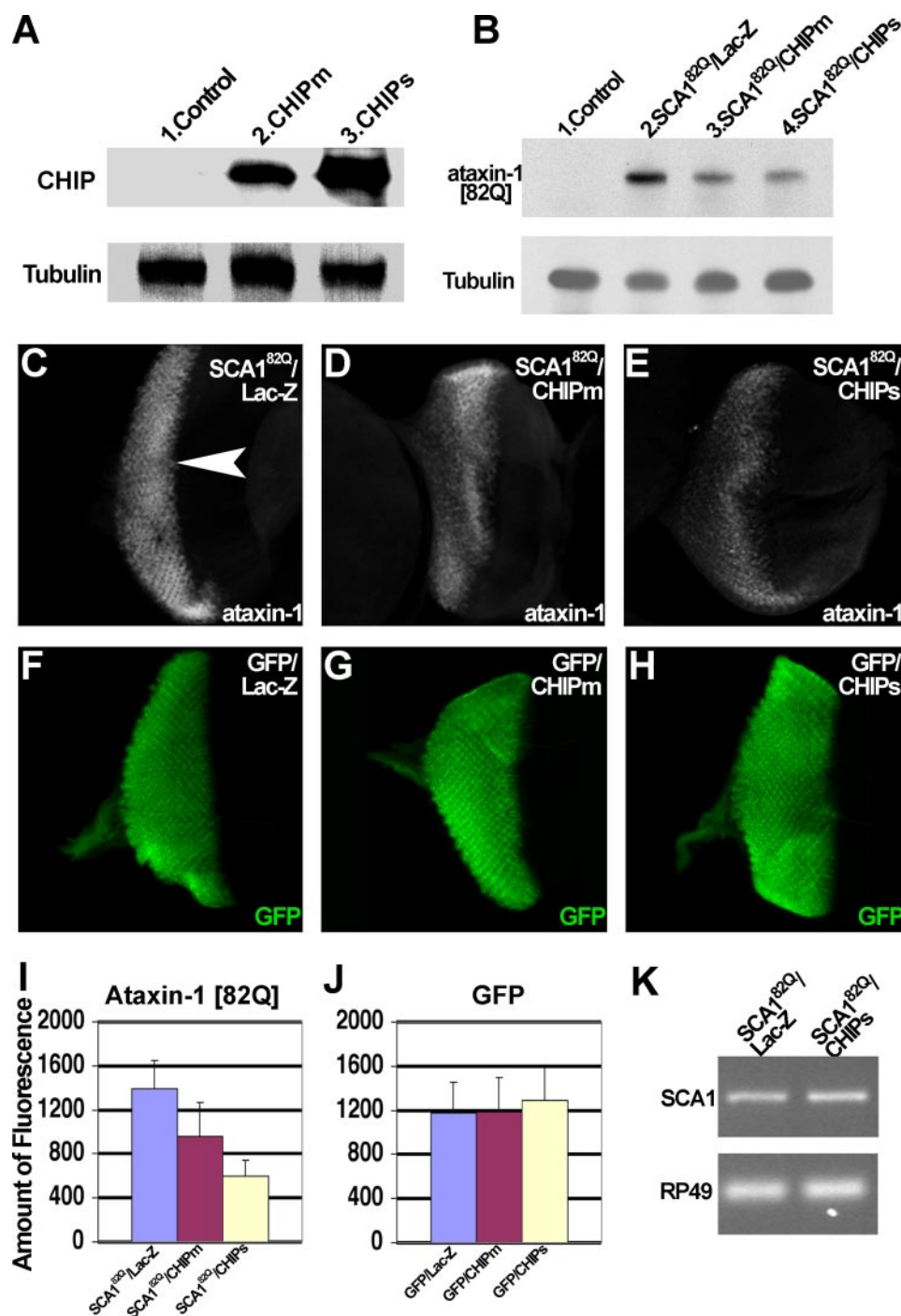


FIGURE 4. CHIP overexpression reduces the steady-state levels of expanded ataxin-1 in *Drosophila*. *A*, immunoblot showing the expression levels of CHIPm versus CHIPs transgenic lines in the eye (five fly heads per lane). Notice the higher levels of CHIP in lane 3 (CHIPs) than in lane 2 (CHIPm). Blots were sequentially probed with rabbit anti-CHIP and mouse anti-tubulin (used as a loading control). *B*, Western blot showing the levels of ataxin-1 [82Q] present in larval eye imaginal discs (EIDs) from age matched animals of the indicated genotype combinations driven by *gmr-GAL4*. Blots were sequentially probed with rabbit anti-ataxin-1 (11NQ) and mouse anti-tubulin (used as a loading control). Lane 1, no ataxin-1 signal detected in control EIDs. Lane 2, normal ataxin-1 [82Q] levels present following co-expression of SCA1^{82Q} and a neutral LacZ transgene in the EIDs. Lanes 3 and 4, progressive decrease of ataxin-1 [82Q] levels when co-expressed with either CHIPm or CHIPs, respectively, in the larval EIDs (ratio lane 2/lane 3 = 1.5, ratio lane 2/lane 4 = 2.5). *C–E*, anti-ataxin-1 immunofluorescence staining; *I*, quantification of anti-ataxin-1 signal, on EIDs expressing SCA1^{82Q} and different levels of CHIP. *C*, EIDs co-expressing SCA1^{82Q} and LacZ show ataxin-1 staining that extends from the morphogenetic furrow (arrowhead) to the most posterior part of the disc. Co-expression of either CHIPm (*D*) or CHIPs (*E*) with SCA1^{82Q} causes a decrease in the intensity of the ataxin-1 signal (compare *C* with *D* and *E* and see quantification in *I*). CHIPs causes a greater decrease in the ataxin-1 signal than CHIPm (compare *D* with *E* and see *I*, $p < 0.01$ for CHIPm and $p < 0.001$ for CHIPs analyzed by Student's *t* test). *F–H*, anti-GFP immunofluorescence staining; *J*, quantification of GFP signal intensity on EIDs expressing the genotypes indicated on top. Neither CHIPm nor CHIPs decrease the intensity of GFP compared with the control (compare *F* with *G* and *H* and see quantification in *J*). *K*, semiquantitative RT-PCR performed on EIDs of the indicated genotypes. Expression of CHIP does not cause a change in the amount of the SCA1 mRNA transcript. RP-49 was used as a loading control for the reaction. Genotypes are as follows: Control, *yw*; *gmr-GAL4/+*; *UAS-LacZ/+*. CHIPm, *yw*; *gmr-GAL4/+*; *UAS-CHIPm/+*. CHIPs, *yw*; *gmr-GAL4/+*; *UAS-CHIPs*. SCA1^{82Q}/LacZ, *UAS-SCA1^{82Q}[F7]/yw*; *gmr-GAL4/+*; *UAS-LacZ/+*. SCA1^{82Q}/CHIPm, *UAS-SCA1^{82Q}[F7]/yw*; *gmr-GAL4/+*; *UAS-CHIPm/+*. SCA1^{82Q}/CHIPs, *UAS-SCA1^{82Q}[F7]/yw*; *gmr-GAL4/+*; *UAS-CHIPs*. GFP/LacZ, *gmr-GAL4*, *UAS-CD8:GFP/+*; *UAS-LacZ/+*. GFP/CHIPm, *gmr-GAL4*, *UAS-CD8:GFP/+*; *UAS-CHIPm/+*. GFP/CHIPs, *gmr-GAL4*, *UAS-CD8:GFP/+*; *UAS-CHIPs*.

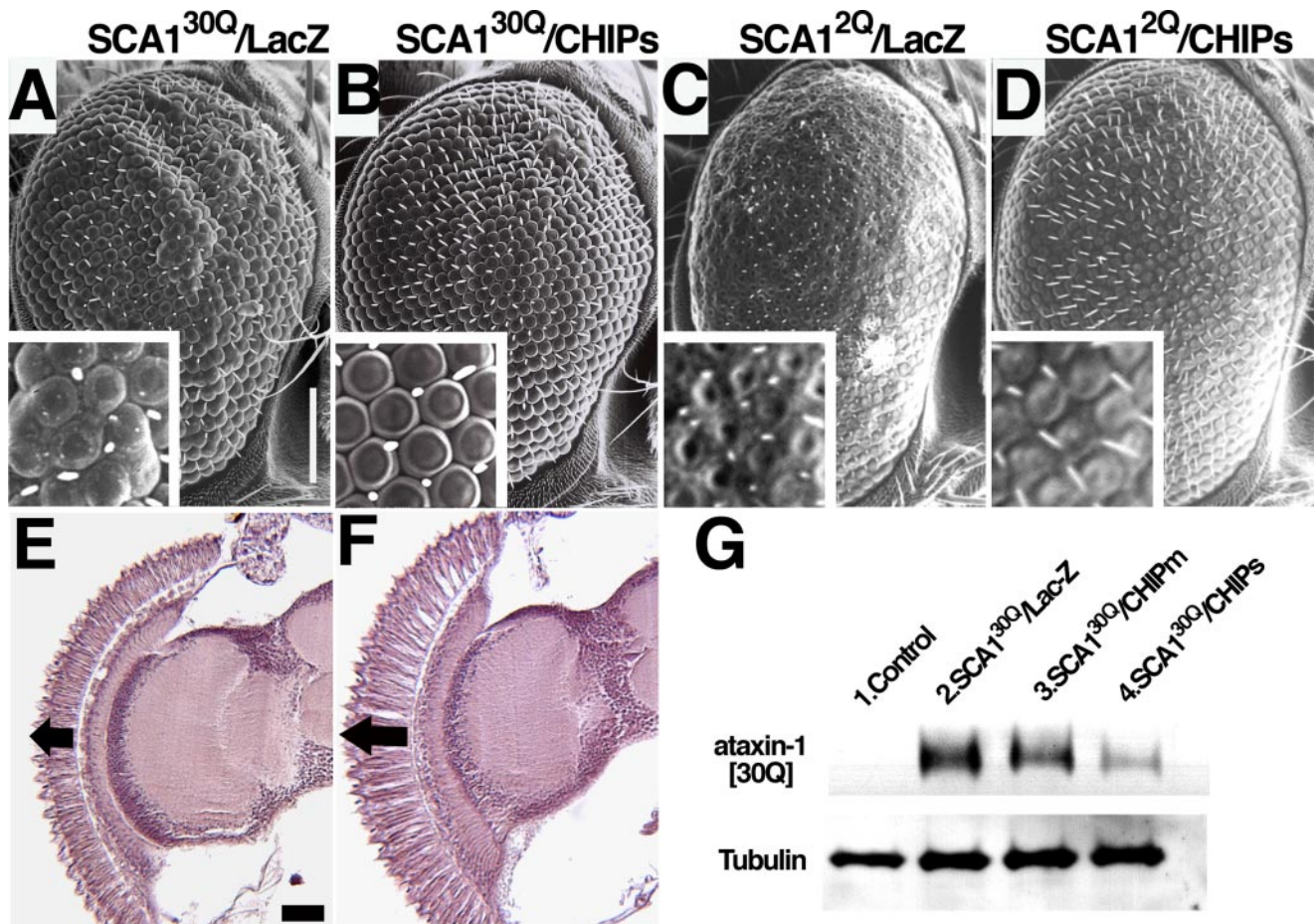


FIGURE 5. CHIP suppresses the eye degeneration induced by unexpanded ataxin-1 and decreases its levels in *Drosophila*. A and B, SEM images; E and F, horizontal paraffin sections of eyes expressing human unexpanded SCA1^{30Q} with either a control transgene (*LacZ*) or with *CHIPs* (genotype combinations indicated on top). Eyes expressing unexpanded SCA1^{30Q} at levels four times higher than the SCA1^{30Q} line shown in Fig. 3 have a relatively mild ommatidial disorganization (A, compare with Fig. 3A); however, they show a reduction in retinal depth similar to the line expressing SCA1^{82Q} (compare E with Fig. 3, E and F). Co-expression of *CHIPs* with SCA1^{30Q} causes a suppression of both external eye and retinal phenotypes (B and F). C and D, SEM images of flies expressing SCA1^{2Q} with either a control transgene (*LacZ*) or with *CHIPs*. SCA1^{2Q} eyes show severe ommatidial and bristle disorganization phenotypes (C, compare with Fig. 3A). The UAS-SCA1^{2Q} line shown expresses six times higher levels than the UAS-SCA1^{82Q} line used in Fig. 3B (data not shown) but causes a similar eye phenotype. Co-expression of *CHIPs* together with SCA1^{2Q} suppresses the ataxin-1 [2Q]-induced phenotype. Notice the improvement in ommatidial and bristle phenotypes (compare C and D). G, Western blot showing unexpanded ataxin-1 [30Q] protein levels in fly eyes expressing the genotype combinations indicated on top. Ataxin-1 is detected with rabbit anti-ataxin-1 (11NQ); mouse anti-tubulin was used as loading control. Lane 1, no ataxin-1 signal detected in control eyes. Lane 2, ataxin-1 [30Q] protein levels present in eyes co-expressing SCA1^{30Q} and *LacZ*. Notice a decrease in ataxin-1 [30Q] levels, in eyes from animals co-expressing SCA1^{82Q} and either *CHIPm* or *CHIPs* (lanes 3 and 4, respectively). The genotypes are as follows; SCA1^{30Q}/*LacZ*, UAS-SCA1^{30Q}[F1]/yw; *gmr*-GAL4/+; UAS-*LacZ*/+; SCA1^{30Q}/*CHIPm*, UAS-SCA1^{30Q}[F1]/yw; *gmr*-GAL4/+; UAS-*CHIPm*/+; SCA1^{30Q}/*CHIPs*, UAS-SCA1^{30Q}[F1]/yw; *gmr*-GAL4/UAS-*CHIPs*; SCA1^{2Q}/*LacZ*, UAS-SCA1^{2Q}[F5]/yw; *gmr*-GAL4/+; UAS-*LacZ*/+; SCA1^{2Q}/*CHIPs*, UAS-SCA1^{2Q}[F5]/yw; *gmr*-GAL4/UAS-*CHIPs*. Scale bar in A–D = 100 μ m; insets are 50 \times 50 μ m. Scale bar in E and F = 10 μ m. A and B, done at 29 °C. C–F, done at 27 °C.

expresses six times more protein and causes a slightly more severe phenotype than the SCA1^{82Q} line (Fig. 5C). Co-expression of *CHIPs* suppresses both the external eye and retinal phenotypes caused by SCA1^{30Q} (Fig. 5, B and F) and the external phenotype of SCA1^{2Q} (Fig. 5D).

We also monitored ataxin-1 [30Q] levels in eye discs co-expressing SCA1^{30Q} and *LacZ* or SCA1^{30Q} and different levels of *CHIP*. Like in the case of ataxin-1 [82Q], *CHIP* expression leads to a decrease in the amount of unexpanded ataxin-1 [30Q]. This decrease was again inversely correlated to the amount of *CHIP* being co-expressed (Fig. 5G).

Protein Context Is Important for *CHIP* Protection against Polyglutamine-induced Neurotoxicity—The observations that *CHIP* protects against both expanded and unexpanded ataxin-1-triggered neurodegeneration suggest that the protein backbone is important for neuroprotection mediated by *CHIP*.

We compared the ability of *CHIP* to protect from similarly expanded polyglutamine tracts in the context of different protein backbones. First we tested a virtually bare polyglutamine tract with only a short hemagglutinin tag as a backbone. Expression of the 127Q-*HA* transgene in the eye causes a strong external phenotype (33) with severe ommatidial disorganization and bristle loss (Fig. 6A). Internally, these eyes present severe retinal degeneration with abundant vacuolization (Fig. 6C). Fig. 6, B and D, show no detectable amelioration of the 127Q-*HA* external and internal eye phenotypes following *CHIP* overexpression. We also tested expression of a similar 128Q tract in the context of an N-terminal fragment of the huntingtin protein containing amino acids 1–276 (NT-Htt[128Q]). Expression of NT-Htt[128Q] in the eye causes no visible external phenotype (data not shown). However, internally NT-Htt[128Q] causes progressive retinal degeneration with severe vacuolization (Fig.

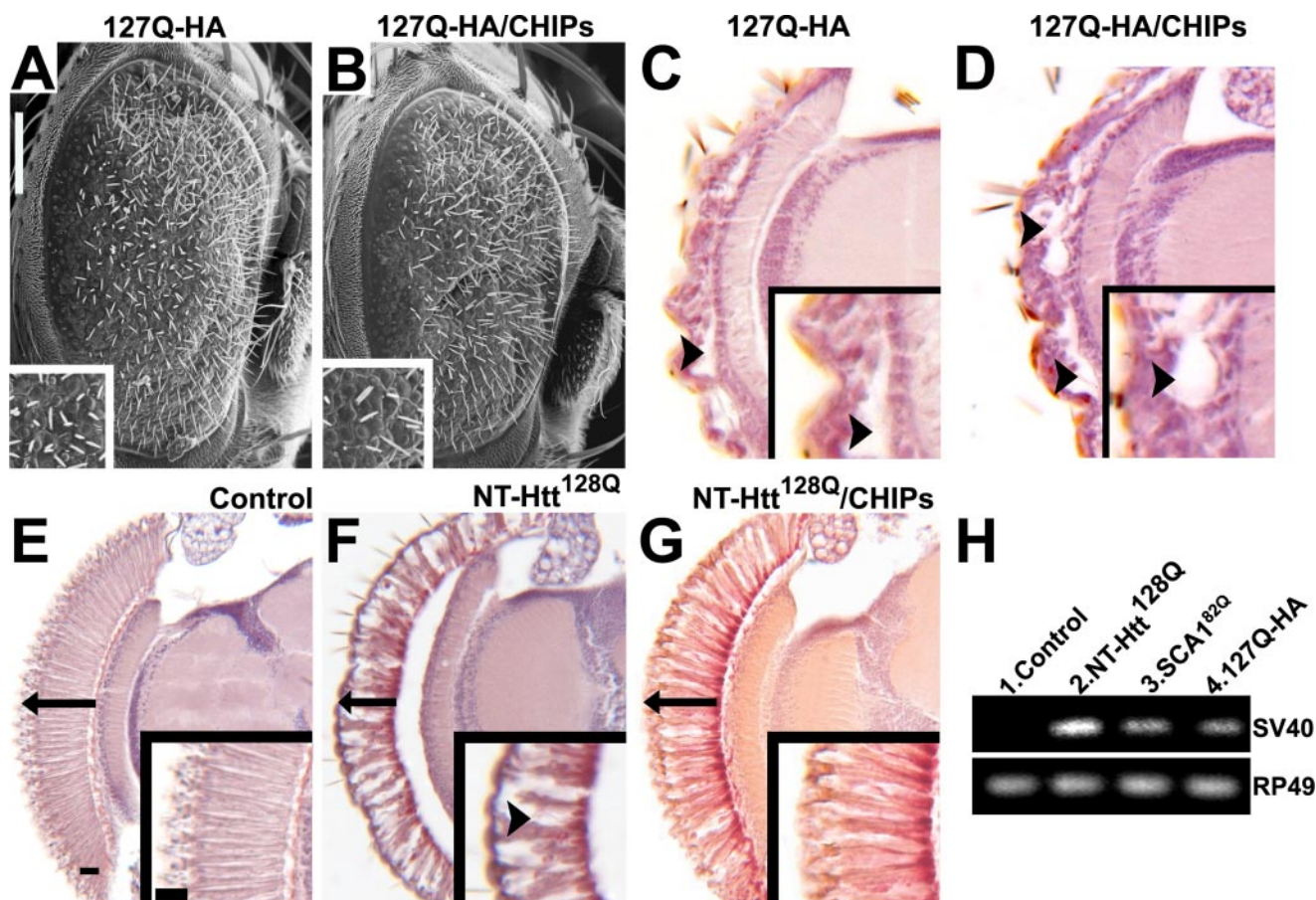


FIGURE 6. Protein context is important for CHIP protection against polyglutamine-induced neurotoxicity. A and B, SEM images of *Drosophila* eyes co-expressing a transgene encoding hemagglutinin-tagged 127Q (127Q-HA) and either GFP (A) or CHIPs (B). Expression of 127Q-HA causes a glassy external eye phenotype and severe ommatidial disorganization. Co-expressing CHIPs together with the 127Q-HA transgene does not modify this phenotype. C and D, horizontal paraffin sections of eye retinas from flies of the same genotypes as A and B. C, 127Q-HA expression causes severe retinal degeneration with abundant vacuolization (arrowheads). Compare with control in E. D, co-expression of CHIPs does not modify 127Q-HA-induced retinal degeneration (compare C and D and insets). E–G, horizontal paraffin sections of eyes from control flies (E) or eyes co-expressing the N-terminal region (amino acids 1–276) of expanded human Huntingtin (NT-Htt^{128Q}) with either GFP (F) or CHIPs (G). All retinas are from 5-day-old animals. Retinas co-expressing NT-Htt^{128Q} and GFP reveal a severe degeneration manifested as a reduction in the depth of the retina (see arrow in F) and abundant vacuolization (inset in F, arrowhead), when compared with control retinas (E). Co-expression of CHIPs together with NT-Htt^{128Q} suppresses the phenotype shown in F. Note the dramatic improvement in retinal depth (arrow) and vacuolization phenotypes (G and inset). H, semiquantitative RT-PCR performed on control eyes or eyes expressing NT-Htt^{128Q}, SCA1^{82Q}, or 127Q-HA. RT-PCR was designed to detect the SV40 transcription termination sequence, which is present in the three transcripts (part of the pUAST vector). RP49 was used as loading control. Lane 1 shows the absence of SV40-containing transcripts. Comparison of lanes 2–4 shows that NT-Htt^{128Q} (lane 2) is expressed at higher levels than SCA1^{82Q} (lane 3) or 127Q-HA (lane 4), which have similar levels of expression. Genotypes are as follows for each panel: A and C, *yw; gmr-GAL4, UAS-127Q-HA/UAS-eGFP; +*; B and D, *yw; gmr-GAL4, UAS-127Q-HA/UAS-CHIPs; +*; E, *yw; gmr-GAL4/+*; F, *yw; gmr-GAL4/UAS-eGFP; UAS-NT-Htt[128Q]/+*; G, *yw; gmr-GAL4/+*; UAS-NT-Htt[128Q]/UAS-CHIPs; H, control: *Rh1-GAL4/+*; NT-Htt^{128Q}: *Rh1-GAL4/+*; SCA1^{82Q}: *Rh1-GAL4/SCA1^{82Q}[F7]*; 127Q-HA: *Rh1-GAL4/+*; UAS-127Q-HA/+.

6, compare F with E). Fig. 6G show that CHIP is able to strongly ameliorate the retinal phenotypes caused by expression of NT-Htt^{128Q} in the eye.

The different effects of CHIP on ataxin-1 [82Q], NT-Htt^{128Q}, or 127Q-HA toxicities may be caused by differences in the expression levels of the respective transgenes. To investigate this possibility we performed semiquantitative RT-PCR analysis of 1-day-old flies expressing these transgenes from the adult eye driver *Rh1-GAL4*. This driver was used to avoid quantification artifacts caused from cell loss that occurs because of the relatively early expression of the toxic transgenes when using *Gmr-GAL4*. Fig. 6H shows that 127Q-HA, the most toxic transgene, is expressed at a lower level than the SCA1^{82Q} or NT-Htt^{128Q} transgenes. Thus, the expression level of 127Q-HA does not explain the failure of CHIP to suppress its toxicity.

The different effects of CHIP on ataxin-1 [82Q], NT-Htt^{128Q}, or 127Q-HA toxicities is, more likely, a consequence of differences among the backbones of these polyglutamine polypeptides. In contrast to the ataxin-1 [82Q] and NT-Htt^{128Q} polypeptides, 127Q-HA does not contain a lysine residue for ubiquitination. These findings emphasize the importance of appropriate protein context for polyglutamine-induced neurodegeneration.

DISCUSSION

CHIP plays a critical regulatory function in the protein quality control machinery of the cell (14, 15) and has been implicated in the pathology of several neurological disorders characterized by protein misfolding and aggregation (22–29).

Here we investigate the relationship between CHIP and ataxin-1 and its relevance for SCA1 pathogenesis. We find that CHIP interacts with expanded ataxin-1 in Co-IP assays and is recruited to ataxin-1 NIs in cell culture. More importantly, CHIP also localizes to the ataxin-1 NIs present in human SCA1 neurons from post-mortem tissue. CHIP ubiquitinates expanded ataxin-1 *in vitro* and in cell culture and Hsp70 enhances this activity. However, we cannot detect ataxin-1 ubiquitination with a CHIP protein carrying a mutation in the TPR domain that is known to mediate interactions with chaperones (16). Thus, it appears that chaperone interaction is essential for CHIP ubiquitination function *in vivo*. It has been reported that CHIP interacts with and enhances the activity of other E3 ligases (34), raising the possibility that *in vivo* ataxin-1 ubiquitination is mediated by an E3 ligase other than CHIP. To investigate this possibility we used a CHIP^{U-box} mutant lacking E3 ligase activity. This CHIP mutant fails to induce ataxin-1 ubiquitination indicating that CHIP directly ubiquitinates ataxin-1. Next we asked whether increased activity of CHIP is able to modify a neurodegenerative phenotype caused by expanded ataxin-1 in a *Drosophila* model of SCA1. We found that CHIP overexpression dramatically decreases expanded ataxin-1-induced toxicity in the *Drosophila* eye. The degree of suppression is higher with increasing levels of CHIP. In accordance with the cell culture ubiquitination data, we find that higher amounts of CHIP lead to lower levels of expanded ataxin-1 in *Drosophila* as determined by immunofluorescence quantification and Western blot analysis.

Taken together these observations indicate that CHIP plays a protective role in SCA1 neuropathology by targeting expanded ataxin-1 for proteasomal degradation in a chaperone dependent manner. These findings are consistent with previous reports implicating CHIP as a protective factor of other polyglutamine proteins by promoting proteasomal degradation (27) and reducing aggregation (26).

Expansion of poly-Q tracts are thought to cause aberrant conformations leading to exposure of hydrophobic residues in the corresponding proteins. Chaperones identify and bind these misfolded proteins in an effort to refold them to their native non-toxic conformations (12, 13). Interestingly, we find that CHIP not only interacts with expanded ataxin-1 but also with the unexpanded isoform in co-IP experiments. This unexpected observation suggests that ataxin-1 can misfold into a toxic conformation even in the absence of the poly-Q expansion. In addition CHIP ubiquitinates unexpanded ataxin-1, and this activity is enhanced by Hsp70. In contrast to ataxin-1, CHIP differentially binds to and enhances the degradation of expanded ataxin-3 or huntingtin but not their unexpanded counterparts (27). Thus unlike other poly-Q proteins, wild-type ataxin-1 may adopt a misfolded toxic conformation that is perhaps stabilized by the poly-Q expansion. In support of this idea unexpanded ataxin-1, unlike normal ataxin-3 or huntingtin, aggregates and triggers neurodegeneration when expressed at high enough levels (10). These and other observations (2, 3, 11, 35, 36) implicate normal function of ataxin-1 in SCA1 pathogenesis, and they also suggest that protein context is important for poly-Q-induced neurodegeneration.

We used *Drosophila* to compare the effects of CHIP on either a pure 127Q tract or an N-terminal huntingtin with a 128Q expansion. While we could not detect amelioration of the toxicity caused by the 127Q tract, CHIP strongly suppresses the 128Q-huntingtin phenotype. The dramatic difference in the ability of CHIP to protect against neurotoxicity caused by similarly expanded poly-Q tracts emphasizes the importance of the protein context in polyglutamine-induced neurodegeneration. These data should be considered when interpreting the results of poly-Q models that lack an appropriate protein context. These models may not recapitulate important features of the human disease, e.g. residues in the corresponding proteins that are required for ubiquitination, phosphorylation, or other post-translational modifications.

In conditional mouse models of SCA1 and Huntington disease, halting expression of the polyglutamine-encoding transcript can lead to recovery of the neurodegenerative process (37, 38). These findings and the discovery of powerful genetic suppressors of polyglutamine-induced neurotoxicity such as CHIP make the prospects for future treatment for SCA1 and other polyglutamine diseases brighter than ever.

Acknowledgments—We thank the Baylor College of Medicine Mental Retardation and Developmental Disabilities Research Center core facilities (HD24062) and B. Antalffy for sectioning and staining the human material, J. Barrish for help with the SEM, R. Atkinson for advice with confocal microscopy, P. Kazemi-Esfarjani for the UAS-127Q-HA strain, and the Bloomington Stock Center for many other *Drosophila* strains.

REFERENCES

1. Zoghbi, H. Y., and Orr, H. T. (2000) *Annu. Rev. Neurosci.* **23**, 217–247
2. Gatchel, J. R., and Zoghbi, H. Y. (2005) *Nat. Rev. Genet.* **6**, 743–755
3. Tsuda, H., Jafar-Nejad, H., Patel, A. J., Sun, Y., Chen, H. K., Rose, M. F., Venken, K. J., Botas, J., Orr, H. T., Bellen, H. J., and Zoghbi, H. Y. (2005) *Cell* **122**, 633–644
4. Klement, I. A., Skinner, P. J., Kaytor, M. D., Yi, H., Hersch, S. M., Clark, H. B., Zoghbi, H. Y., and Orr, H. T. (1998) *Cell* **95**, 41–53
5. Matilla, A., Roberson, E. D., Banfi, S., Morales, J., Armstrong, D. L., Burright, E. N., Orr, H. T., Sweatt, J. D., Zoghbi, H. Y., and Matzuk, M. M. (1998) *J. Neurosci.* **18**, 5508–5516
6. Ciechanover, A., and Brundin, P. (2003) *Neuron* **40**, 427–446
7. Cummings, C. J., Mancini, M. A., Antalffy, B., DeFranco, D. B., Orr, H. T., and Zoghbi, H. Y. (1998) *Nat. Genet.* **19**, 148–154
8. Cummings, C. J., Reinstein, E., Sun, Y., Antalffy, B., Jiang, Y., Ciechanover, A., Orr, H. T., Beaudet, A. L., and Zoghbi, H. Y. (1999) *Neuron* **24**, 879–892
9. Cummings, C. J., Sun, Y., Opal, P., Antalffy, B., Mestrl, R., Orr, H. T., Dillmann, W. H., and Zoghbi, H. Y. (2001) *Hum. Mol. Genet.* **10**, 1511–1518
10. Fernandez-Funez, P., Nino-Rosales, M. L., de Gouyon, B., She, W. C., Luchak, J. M., Martinez, P., Turiegano, E., Benito, J., Capovilla, M., Skinner, P. J., McCall, A., Canal, I., Orr, H. T., Zoghbi, H. Y., and Botas, J. (2000) *Nature* **408**, 101–106
11. Mizutani, A., Wang, L., Rajan, H., Vig, P. J., Alaynick, W. A., Thaler, J. P., and Tsai, C. C. (2005) *EMBO J.* **24**, 3339–3351
12. Ma, Y., and Hendershot, L. M. (2001) *Cell* **107**, 827–830
13. Wickner, S., Maurizi, M. R., and Gottesman, S. (1999) *Science* **286**, 1888–1893
14. Cyr, D. M., Hohfeld, J., and Patterson, C. (2002) *Trends Biochem. Sci.* **27**, 368–375
15. Wiederkehr, T., Bukau, B., and Buchberger, A. (2002) *Curr. Biol.* **12**,

R26–R28

16. Ballinger, C. A., Connell, P., Wu, Y., Hu, Z., Thompson, L. J., Yin, L. Y., and Patterson, C. (1999) *Mol. Cell. Biol.* **19**, 4535–4545
17. Jiang, J., Ballinger, C. A., Wu, Y., Dai, Q., Cyr, D. M., Hohfeld, J., and Patterson, C. (2001) *J. Biol. Chem.* **276**, 42938–42944
18. Murata, S., Chiba, T., and Tanaka, K. (2003) *Int. J. Biochem. Cell Biol.* **35**, 572–578
19. Hatakeyama, S., Matsumoto, M., Yada, M., and Nakayama, K. I. (2004) *Genes Cells* **9**, 533–548
20. Kampinga, H. H., Kanon, B., Salomons, F. A., Kabakov, A. E., and Patterson, C. (2003) *Mol. Cell. Biol.* **23**, 4948–4958
21. Dai, Q., Zhang, C., Wu, Y., McDonough, H., Whaley, R. A., Godfrey, V., Li, H. H., Madamanchi, N., Xu, W., Neckers, L., Cyr, D., and Patterson, C. (2003) *EMBO J.* **22**, 5446–5458
22. Urushitani, M., Kurisu, J., Tateno, M., Hatakeyama, S., Nakayama, K., Kato, S., and Takahashi, R. (2004) *J. Neurochem.* **90**, 231–244
23. Shin, Y., Klucken, J., Patterson, C., Hyman, B. T., and McLean, P. J. (2005) *J. Biol. Chem.* **280**, 23727–23734
24. Shimura, H., Schwartz, D., Gygi, S. P., and Kosik, K. S. (2004) *J. Biol. Chem.* **279**, 4869–4876
25. Petrucelli, L., Dickson, D., Kehoe, K., Taylor, J., Snyder, H., Grover, A., De Lucia, M., McGowan, E., Lewis, J., Prihar, G., Kim, J., Dillmann, W. H., Browne, S. E., Hall, A., Voellmy, R., Tsuboi, Y., Dawson, T. M., Wolozin, B., Hardy, J., and Hutton, M. (2004) *Hum. Mol. Genet.* **13**, 703–714
26. Miller, V. M., Nelson, R. F., Gouvion, C. M., Williams, A., Rodriguez-Lebron, E., Harper, S. Q., Davidson, B. L., Rebagliati, M. R., and Paulson, H. L. (2005) *J. Neurosci.* **25**, 9152–9161
27. Jana, N. R., Dikshit, P., Goswami, A., Kotliarova, S., Murata, S., Tanaka, K., and Nukina, N. (2005) *J. Biol. Chem.* **280**, 11635–11640
28. Hatakeyama, S., Matsumoto, M., Kamura, T., Murayama, M., Chui, D. H., Planel, E., Takahashi, R., Nakayama, K. I., and Takashima, A. (2004) *J. Neurochem.* **91**, 299–307
29. Choi, J. S., Cho, S., Park, S. G., Park, B. C., and Lee do, H. (2004) *Biochem. Biophys. Res. Commun.* **321**, 574–583
30. Brand, A. H., and Perrimon, N. (1993) *Development (Camb.)* **118**, 401–415
31. Chen, H. K., Fernandez-Funez, P., Acevedo, S. F., Lam, Y. C., Kaytor, M. D., Fernandez, M. H., Aitken, A., Skoulakis, E. M., Orr, H. T., Botas, J., and Zoghbi, H. Y. (2003) *Cell* **113**, 457–468
32. Zhang, M., Windheim, M., Roe, S. M., Pegg, M., Cohen, P., Prodromou, C., and Pearl, L. H. (2005) *Mol. Cell.* **20**, 525–538
33. Kazemi-Esfarjani, P., and Benzer, S. (2000) *Science* **287**, 1837–1840
34. Imai, Y., Soda, M., Hatakeyama, S., Akagi, T., Hashikawa, T., Nakayama, K. I., and Takahashi, R. (2002) *Mol. Cell.* **10**, 55–67
35. Tsai, C. C., Kao, H. Y., Mitzutani, A., Banayo, E., Rajan, H., McKeown, M., and Evans, R. M. (2004) *Proc. Natl. Acad. Sci. U. S. A.* **101**, 4047–4052
36. Emamian, E. S., Kaytor, M. D., Duvick, L. A., Zu, T., Tousey, S. K., Zoghbi, H. Y., Clark, H. B., and Orr, H. T. (2003) *Neuron* **38**, 375–387
37. Zu, T., Duvick, L. A., Kaytor, M. D., Berlinger, M. S., Zoghbi, H. Y., Clark, H. B., and Orr, H. T. (2004) *J. Neurosci.* **24**, 8853–8861
38. Yamamoto, A., Lucas, J. J., and Hen, R. (2000) *Cell* **101**, 57–66

CHIP Protects from the Neurotoxicity of Expanded and Wild-type Ataxin-1 and Promotes Their Ubiquitination and Degradation

Ismael Al-Ramahi, Yung C. Lam, Hung-Kai Chen, Beatrice de Gouyon, Minghang Zhang, Alma M. Pérez, Joana Branco, Maria de Haro, Cam Patterson, Huda Y. Zoghbi and Juan Botas

J. Biol. Chem. 2006, 281:26714-26724.

doi: 10.1074/jbc.M601603200 originally published online July 10, 2006

Access the most updated version of this article at doi: [10.1074/jbc.M601603200](https://doi.org/10.1074/jbc.M601603200)

Alerts:

- [When this article is cited](#)
- [When a correction for this article is posted](#)

[Click here](#) to choose from all of JBC's e-mail alerts

Supplemental material:

<http://www.jbc.org/content/suppl/2006/07/11/M601603200.DC1>

This article cites 38 references, 15 of which can be accessed free at

<http://www.jbc.org/content/281/36/26714.full.html#ref-list-1>